ELSEVIER

The diurnal cycle and the meridional extent of the tropics

Paul A. Milewski [a,*], Esteban G. Tabak [b]

[a] *Department of Mathematics, University of Wisconsin, Madison, 480 Lincoln Dr., Madison, WI 53706, United States*
[b] *Courant Institute of Mathematical Sciences, New York University, 251 Mercer St., New York, NY 10012, United States*

ARTICLE INFO

ABSTRACT

An explanation is proposed for the meridional extent of the Hadley cells: the diurnal waves forced by solar heating trapped between $-30°$ and $30°$. These baroclinic waves, we propose, give rise to the daily nature of tropical meteorology, and ultimately to the intensified mixing and circulation associated with the Hadley cells and the shape of the tropopause. This conceptual explanation is validated with basic scaling arguments and with two diurnally forced one-layer models: One linear and the other nonlinear, the latter with a simple closure for mixing and entrainment by breaking waves.

© 2010 Elsevier B.V. All rights reserved.

1. Introduction

The Hadley cells are arguably the most prominent feature of the troposphere, and define the extent of the tropics. They are two large mean circulation cells, driven by the differential insolation between the tropics and the mid-latitudes. Moist air rises in a relatively thin strip, the Intertropical Convergence Zone (ITCZ), through deep convective storms, losing most of its water content through precipitation. In the upper troposphere, the air travels toward higher latitudes, north and south. By conservation of angular momentum, it thus generates increasingly strong westerly winds, which peak as high-altitude subtropical jets. Then the air subsides in an area confined around the 30° parallels, the Horse latitudes; these descending dry air masses are responsible for the majority of the deserts on Earth. Finally, the air travels back toward the ITCZ near the Earth's surface, producing in the process, again by conservation of angular momentum, the easterly trade winds. The tropics, equatorwards of 30°, display a strong diurnal signal in the wind, pressure and temperature, often marked by regular daily storms. Polewards of 30°, the weather systems have longer spatio-temporal scales.

The location of the ITCZ travels seasonally, northward during the northern summer, and southward during the northern winter. The Hadley cell is stronger in the winter hemisphere, since the imbalance of solar radiation there between the ITCZ and the winter 30th parallel is much more accentuated [1]. Yet the outer edges of the cells are invariably at a latitude close to 30°, north and south.

It is the cells that give the tropopause, the boundary between the stratosphere and the troposphere, its characteristic "hat-shaped" profile, with a height of about 16 km in the tropics, descending sharply to about 9 km in the extratropical zone. This paper provides a simple conceptual explanation for such permanent and sharply-defined meridional extent of the tropical troposphere.

In what is currently one of the most widely accepted explanation, due to Held and Hou [2,3], the location of the outer edges of the cells depends on the intensity and meridional distribution of the atmospheric heating. Thus, if the heating parameters should change, as they would in a global warming scenario, the location of the edges could change as well, as has been argued in recent literature [4–7]. In our explanation, however, the edge's location at 30° follows from first principles, so it would not be affected significantly by climate change. It is the height and stratification profile of the tropical troposphere that can evolve, not its meridional extent.

Our explanation starts with the forcing that drives the cells. The reason that there are Hadley cells – and, in fact, that there is a troposphere at all – is that the sun heats the atmosphere from below. The atmosphere is, to leading order, transparent to direct solar radiation, yet the ground and sea water are not: they absorb a significant fraction, and re-emit it in the form of infrared radiation and advection of air parcels carrying sensible and latent heat. Heating a fluid from below gives rise to instability; in the atmospheric scenario, to convective cells, tropical storms and, more generally, to the stirring and mixing of air masses that yields the tropical troposphere.

Solar heating has a period of one day, an elementary fact that is forgotten nonetheless in most theories of atmospheric circulation. This diurnal heating acts as a periodic forcing on a stratified fluid medium, and therefore yields disturbances – gravity waves – with the same period of one day. In a rotating environment, gravity

* Corresponding author.
E-mail addresses: milewski@math.wisc.edu (P.A. Milewski), tabak@cims.nyu.edu (E.G. Tabak).

waves have a minimal frequency given by the absolute value of the Coriolis parameter f, which, on a rotating spherical planet, adopts the form

$$f = 2\Omega \sin(\alpha),$$

where α is the latitude and

$$\Omega = \frac{2\pi}{1\text{day}}$$

is the frequency of the planet's rotation. Then diurnally forced waves produced by solar heating must satisfy

$$\Omega \geq 2\,\Omega\,|\sin(\alpha)|,$$

which implies that

$$|\alpha| \leq 30°.$$

Hence diurnal gravity waves are trapped in the tropics, in a band between the latitudes of 30° north and south, precisely the band occupied by the Hadley cells.

This simple fact already explains why there is such a clear daily cycle in the wind field in the tropics, absent in the middle and high latitudes. The winds over Africa, for instance, a continent situated almost sharply between $-30°$ and $30°$, change direction and intensity with a daily pattern, unlike the winds over North America, Europe and northern and Central Asia, organized in weather systems with a timescale of roughly five days and a dominant, typically eastward, direction. The observational record over the oceans is less direct – there are fewer weather stations – and the diurnal cycle is thought to be less pronounced. However, recent analysis of data [8,9] indicates the clear presence of a daily cycle in the precipitation over the tropical seas.

To check that interpreting these daily patterns in the tropics in terms of diurnal waves is consistent with observations, we can compute some of the fundamental scales involved. The dominant manifestation of thermal forcing in the tropics is through storms, which are typically associated with the effective moist baroclinic mode of the atmosphere. The corresponding value c of the wave speed [10] is of the order of 15 m/s. For diurnal waves, this yields a length-scale

$$L = c * 1\,\text{day} \approx 1000\,\text{km},$$

a typical meridional distance among tropical storm systems.

This suggests the following rationale for the meridional extent of the tropical troposphere and the Hadley cells. For the air parcels that make up the cells to propagate vertically, they need the atmosphere to be at most weakly stratified, or else the stratification would act as a barrier to vertical motion. This homogenization of the troposphere is achieved by mixing both by the air parcels themselves, with their accompanying turbulent entrainment, and by other processes, such as breaking internal waves and shear instability, all of which require the active participation of waves. The rising parcels, in particular, are not a straightforward response to solar heat: a warm, moist environment at ground level creates the pre-conditions for convection, yet this requires, in order to materialize, the development of areas of low pressure, so that Ekman pumping in the boundary layer can bring about convergence and upwelling. Similarly, areas of high pressure cause air to descend. This alternating pattern of regions of low and high pressure is brought about by waves. Those waves that are diurnal, as argued above, can only propagate in the band between the parallels at $-30°$ and $30°$.

By contrast, the theory in [2] for the extent of the cells can be summarized as follows. In the upper branch of the cells, the air moving away from the equator must preserve angular momentum, yielding the meridional dependence of the zonal wind along this upper branch. If the height of the branch is known, then the

thermal wind relation yields, in an average sense, the meridional dependence of the temperature. With this, one can estimate the amount of thermal radiation out to space. Since the cells exchange heat only weakly with the mid-latitudes, the meridional integral of this outward radiation must match the external heating. This equality sets the meridional extent of the cells. More recently, Held [3] qualified his explanation – see also [11,12] –, adding the constraint that the Hadley cells could not extend into regions with active baroclinicity. However, since the onset of the baroclinic instability depends on the stratification and shear profiles, and these are determined to a large degree by the circulation itself, this constraint alone is not a predictor of the actual meridional extent of the cells.

These theories rely on a number of simplifications, yet we do not argue with their general conclusions, but with the causality that they imply. In the theories, the height of the outward branches of the cells is given (as well as the stratification in the modified theory) and their meridional extent is derived from the energy balance or the onset of baroclinicity. If our theory is correct, it is the meridional extent that is given by dynamical reasons – wave trapping – and so it is the height of the outward branch that needs to adjust accordingly to satisfy energy conservation.

In this paper, we validate our hypothesis through two simple models. The first model is linear, simply intended to display the robustness of the trapping of diurnal waves between $-30°$ and $30°$. The second model – a nonlinear rotating shallow water system where the complex dynamics of mixing is represented through a simple closure, with breaking waves entraining stratospheric air – shows how this trapped wave action may translate into a hat-shaped profile for the tropopause. Both of our models have a single layer representing the first baroclinic mode, and cannot therefore account for the meridional Hadley circulation in the cells nor for a direct description of the depth of the troposphere. It does, however, indicate the latitudinal dependence of the intensity of entrainment and mixing. In a final section, we discuss what ingredients are required of a model so that it can capture the mean circulation as well.

2. A model for trapped tropospheric waves

We propose to validate the hypothesis outlined above through a simple dynamical model with the following ingredients and modeling reductions: [1]

- A meridionally dependent Coriolis parameter

$$f = 2\,\Omega\,\sin(\alpha).$$

- No zonal dependence. Note that this is not the same as taking zonal means, in that the sun still displays its diurnal cycle. One can think of a fixed meridian, with the sun appearing and disappearing daily from the sky, creating a meridional pattern. Clearly real waves span all directions, yet since the baroclinic waves that we study are not fast enough to follow the sun in its path around the Earth – these would be thermal tides, a barotropic phenomenon – their zonal and meridional components are not fundamentally different. Since the waves are trapped meridionally, we use a "one-and-a-half dimensional" modeling reduction, which keeps both meridional *and* zonal components of the wind field, but represents only their meridional dependence.
- Hydrostatically balanced dynamics.

---

[1] The non-specialist reader can find an up-to-date general reference on the fundamental concepts of geophysical fluid dynamics, such as the distinction between barotropic and baroclinic waves, in [13].

- Simplified stratification. We represent the troposphere as a shallow water layer of vertically uniform density bounded below by an the Earth's surface – free of any topography – and above by an infinite passive layer of constant density modeling the stratosphere. In order to capture the meridional circulation in the cells, we would need to include a frictional boundary layer. In this paper, however, we adopt the most distilled model designed only to prove the concept that trapped waves may lead to a discontinuous mean profile.
- An external, meridionally dependent, time periodic forcing of the buoyancy field, mimicking the thermal forcing by the sun.
- A simplified description of mixing and entrainment. We use a closure for stratospheric air entrainment through breaking waves that we developed in [14], valid for subcritical flows. The basic idea is to replace mass by energy conservation. Both are equivalent in smooth parts of the flow but, when shocks develop, energy conservation implies mass growth. This observation is reciprocal to the more conventional one for non-entraining hydraulic jumps and bores, where mass is conserved and energy is dissipated.
- A Boussinesq treatment of density variations. In particular, the effect of heating is modeled as affecting the fluid's density, but not its volume. Hence volume, not mass, is conserved in the presence of heating. This is customarily done in geophysical models. Our motivation here arises from the need to decouple baroclinic and barotropic dynamics. To see this, consider the real effect of heating on the troposphere: it changes the air's density and, if the vertical mean of the heating is nonzero, it consistently raises or lowers the fluid column's height to preserve mass. Yet the latter is a barotropic effect, to which the atmosphere would adjust very rapidly through waves an order of magnitude faster than their baroclinic counterpart; in fact through the barotropic waves responsible for the thermal tides. The Boussinesq model of heating is a simple way of replacing this barotropic component of the dynamics – the global tides – with an effectively infinitely fast mode that re-equilibrates the volume over the spatial scales we consider. Once this modeling hypothesis on heating is used, it is most consistent to combine it with the other reduction bearing Boussinesq's name, which simplifies inertia by defining momentum as consisting of volume – rather than mass – times velocity.

We would like to highlight an important note in the interpretation of the results of our model, resulting from the single layer approximation: that h should be viewed both at the effective height of the first baroclinic mode and, in long-time averages, as a proxy for the height of the troposphere. Clearly h will oscillate with the diurnal frequency and therefore it does not represent the depth of the troposphere at each instant in time, but rather the pressure variations associated with tropical storms. However, the accumulated effect of the associated mixing yields, through the long-time average of h, a reasonable estimate for the profile of the tropopause.

Even though the frequency Ω of the Coriolis parameter and that of the thermal forcing agree on Earth – up to the third of a percent difference between the sidereal and the solar days – the model should allow them to differ, to validate the claim that it is the relation between these two frequencies that determines the extent of the tropics. As a matter of curiosity, the value of one frequency is twice the other's on Venus where, because of the slow and retrograde nature of the planet's rotation, there are two solar days per revolution.

3. Models and results

In our model, the effective moist baroclinic mode of the troposphere has an equivalent height $h(y, t)$ and a density

$$\rho = \rho_s \left(1 + \frac{1}{g} g'(y, t) \right), \tag{1}$$

uniform in the vertical. Here ρ_s is the stratosphere's uniform density, and

$$g' = g \frac{\rho - \rho_s}{\rho_s} > 0,$$

the reduced gravity, is a function of space and time, given by the heating. The pressure above the tropopause is a [linear] function of the height. We often use the terms "reduced gravity" and "buoyancy" interchangeably in this paper.

We write the rotating shallow water system in spherical coordinates, with a variable buoyancy g', in the Boussinesq approximation:

$$h_t + \frac{1}{\cos(y)} [\cos(y) h v]_y = 0 \tag{2}$$

$$(hv)_t + \frac{1}{\cos(y)} \left[\cos(y) h v^2 \right]_y + \left[\frac{1}{2} g' h^2 \right]_y + f(y) h u$$

$$+ \frac{h}{R} u^2 \tan(y) = 0 \tag{3}$$

$$(hu)_t + [hvu]_y - f(y) h v = 0, \tag{4}$$

where h represents the height, v and u the meridional and zonal velocities, R is the radius of the Earth, and all functions depend only on the longitude y and the time t. The buoyancy g' is forced through an equation of the form

$$\frac{dg'}{dt} = g'_t + v g'_y = \lambda(H(y, t) - g'), \tag{5}$$

where H is the external forcing – the time-dependent *radiative equilibrium* profile – and λ a relaxation parameter.

We write the heating function H as a mean buoyancy minus the product of a meridional and a temporally dependent factor,

$$H = 1 - B(y) T(t). \tag{6}$$

The actual temporal dependence of the diurnal forcing is well approximated by a truncated cosine function,

$$T(t) = \left(\max(\cos(2\pi t), 0) \right)^2, \tag{7}$$

where t is measured in days. The origin of this asymmetric form of the temporal dependence is two-fold: the switching off of solar radiation during the night, and the asymmetry of convection, that acts only when the ground is warmer than the air. Simple Fourier analysis yields the spectral decomposition

$$T(t) = \sum_{n=1}^{\infty} T_n \cos(2\pi n t), \tag{8}$$

with

$$T_n = \begin{cases} \dfrac{1}{4} & \text{for } n = 0 \\ \dfrac{1}{8} & \text{for } n = 2 \\ 0 & \text{for } n \text{ even}, n > 2 \\ \dfrac{2}{\pi} \dfrac{(-1)^{\frac{n+1}{2}}}{n(n^2 - 4)} & \text{for } n \text{ odd}. \end{cases} \tag{9}$$
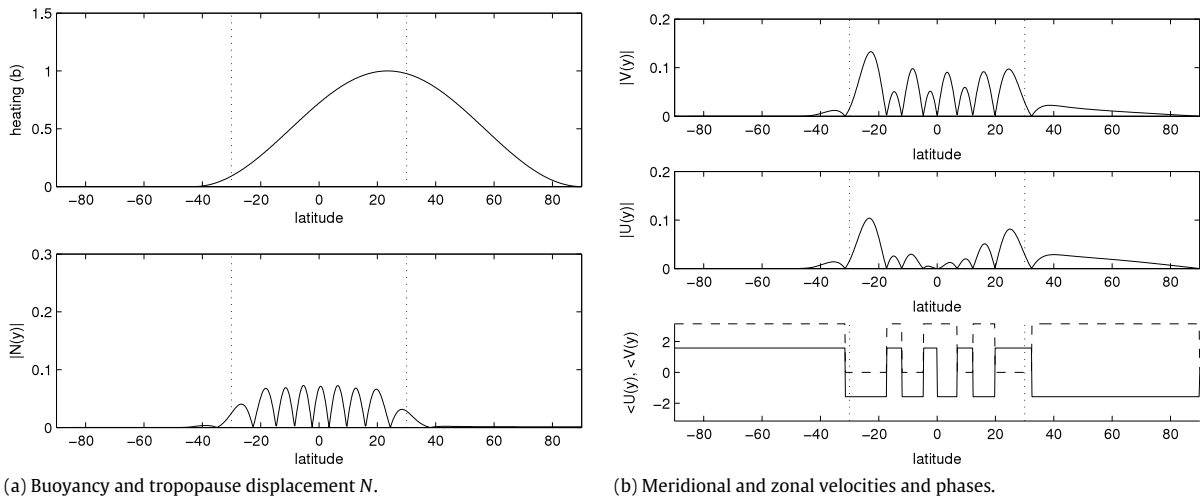
Except for the steady mode $n = 0$, with no dynamics, the dominant mode is $n = 1$. Thus one may consider a simplest model where only this mode is acting. In nonlinear scenarios, we will need to add the mean, $n = 0$, because of its nontrivial meridional dependence.
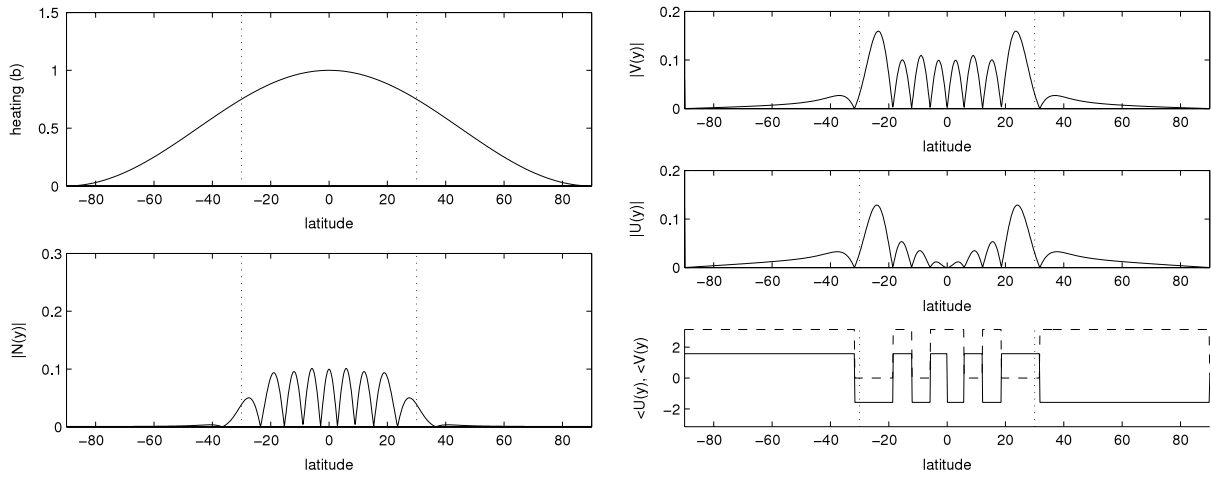
(a) Buoyancy and tropopause displacement N.

(b) Meridional and zonal velocities and phases.

Fig. 1. Linear model at the equinox.

(a) Buoyancy and tropopause displacement N.

(b) Meridional and zonal velocities and phases.

Fig. 2. Linear model at the northern summer solstice.

We adopt a simplified representation of the meridional dependence of the forcing, that captures its main qualitative features without going into unnecessary detail:

$$B(y) = \left[\max \left(\cos \left(\frac{\pi}{2} \frac{y - y_0}{\pi/2 - |y_0|} \right), 0 \right) \right]^2. \tag{10}$$

This function is centered at y_0, a rough representative of seasonal effects: y_0 is zero during the equinoxes, and reaches $\pm 23.5°$ during the solstices. This function, depicted for $y_0 = 0$ and $y_0 = 23.5°$ in Figs. 1(a) and 2(a), is intended to represent mostly the diurnal component of the forcing, hence its zero values at both the summer and the winter poles. Two scenarios will be considered: a frozen scenario where the meridional structure is fixed throughout the year, and another where it changes seasonally—that is, y_0 is a (slow) function of t.

The function $B(y)$ mimics the solar radiation impinging on Earth. One might consider adding the convective response, including for instance an intensification of the forcing at the ITCZ. Yet we prefer to pose a model that does not pre-assume any dynamical response of the atmosphere to the external radiation: it is too tempting, in climate studies, to use observed features of the system to build theories that end up "explaining" these very features! Ideally, a model compatible with a meridional circulation would yield an ITCZ without the need to parameterize it ab initio.

We will adopt two complementary approaches to the Eqs. (2)–(4): in one, we linearize the equations while preserving all the spherical geometric terms. In the other, we keep the nonlinearity but, for simplicity, remove all those factors, except for the meridional variation of the Coriolis parameter. In this second approach, we also replace volume by energy conservation, so as to permit entrainment at breaking waves (no such replacement is necessary in the linear problem, since it has no wave breaking).

3.1. Linear regime

In the linear regime, we adopt $h = h_0 + \eta$, $g' = g_0'(1 - b)$ (the negative sign is to account that an increased buoyancy corresponds to a decrease in reduced gravity), and obtain

$$\eta_t + \frac{h_0}{\cos y}(v \cos y)_y = 0 \tag{11}$$

$$v_t + f(y)u + g_0'\eta_y = \frac{1}{2}g_0'h_0 b_y \tag{12}$$

$$u_t - f(y)v = 0. \tag{13}$$

The equations are nondimensionalized using $c = \sqrt{g_0'h_0}$ as the scaling for the velocities, h_0 as the scaling for the vertical displacement, the inverse of the Earth's rotation rate Ω^{-1} as a

(a) Buoyancy and tropopause displacement N.

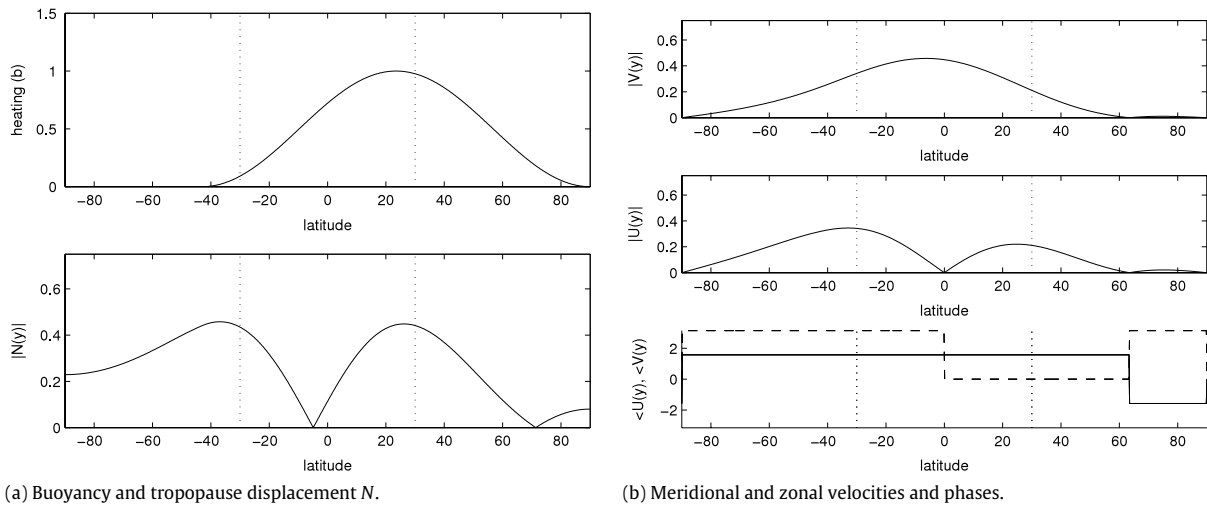(b) Meridional and zonal velocities and phases.

Fig. 3. Linear model for barotropic parameters.

timescale, and the Earth's radius R as the horizontal length-scale. The dimensionless linear equations are then

$$\eta_t + \epsilon \frac{1}{\cos y}(v \cos y)_y = 0 \tag{14}$$

$$v_t + f(y)u + \epsilon \eta_y = \frac{1}{2}\epsilon b_y \tag{15}$$

$$u_t - f(y)v = 0, \tag{16}$$

where f stands for $\frac{f}{\Omega}$, and

$$\epsilon = \frac{c}{R\Omega}.$$

Typical atmospheric values for c are of the order of 15 m/s for the effective moist baroclinic mode. This corresponds to ϵ approximately equal to 0.03, small enough to give rise to multiple-scale phenomena: ϵ can be seen as the quotient between the length-scale of the diurnal waves, roughly 1000 km, and the circumference of the Earth. (An upper bound for baroclinic speeds is approximately 45 m/s, corresponding to the first dry mode and below for higher modes. The corresponding value of ϵ is 0.1, still resulting in wave trapping between $-30°$ and $30°$.)

Next we eliminate the explicit appearance of ϵ in the equations, by rescaling the meridional variable: $y \to \epsilon y$. Yet ϵ still appears in the meridional dependence of the Coriolis parameter f, in the geometrical factor $\cos(\epsilon y)$, and in the location of the boundaries, at $\pm \frac{\pi}{2\epsilon}$.

Since the forced equation for the buoyancy $b(y, t)$ decouples from the flow at the linear level, we can bypass the external heating and consider instead $b(y, t)$ as a given periodic function of frequency ω : $b = B(y)e^{i\omega t}$, where the diurnal case has $\omega = 1$. The solutions to the linear problem have the same frequency, so the transformation $\partial_t \to i\omega$ yields

$$i\omega u - fv = 0 \tag{17}$$

$$\left(i\omega + \frac{f^2}{i\omega}\right)v + \eta_y = \frac{1}{2}b_y \tag{18}$$

$$i\omega \eta + \frac{1}{\cos(\epsilon y)}[v \cos(\epsilon y)]_y = 0. \tag{19}$$

These imply a second order forced equation for v alone:

$$\left[\frac{1}{\cos(\epsilon y)}[v \cos(\epsilon y)]_y\right]_y + (\omega^2 - f^2)v = -\frac{i}{2}\omega b_y. \tag{20}$$

This equation has a turning point when $\omega = f$, i.e. at $30°$ when $\omega = 1$. Equatorwards of this location the solutions are oscillatory, while they decay exponentially poleward. For the meridional dependence $B(y)$, we use (10), with y_0 at either a solstice or an equinox. Most of the examples below have $\omega = 1$, corresponding to the diurnal cycle. For the inverse length-scale, we choose $\epsilon = 0.0324$, corresponding to a typical first baroclinic speed $c = 15$ m/s.

Fig. 1 depict the results when $y_0 = 0$, i.e. with the sun at the equinox. Fig. 1(a) shows the imposed buoyancy $B(y)$, as well as the resulting amplitude for the perturbation height of the troposphere, $\eta(y)$, a wave response trapped between $-30°$ and $30°$. Fig. 1 (b) shows the amplitudes of the meridional and zonal velocities, also trapped in the tropics. The phases of these are also displayed: the zonal velocity is in phase with the buoyancy, and $90°$ away from the meridional velocity, as is characteristic of frictionless rotating flows. The resulting mean values of the winds and height are not captured by the linear dynamics, where all variables oscillate back and forth. Notice the intensification of the winds and decay of the perturbation height as one approaches $30°$, consistent with the extreme non-equipartition of wave energy for gravity waves when $\omega = f$ [15].

Fig. 2 have $y_0 = 23.5°$, with the sun at the northern summer solstice. Even though this makes the forcing highly asymmetric, it has little effect on the waves, which are still trapped between $\pm 30°$ and, if anything, show more activity in the winter hemisphere.

It is still the northern summer in Fig. 3, but this time we are looking at the dynamics of the barotropic mode, with $c = 300$ m/s and $\epsilon \approx 0.6$, no longer small. As a consequence, there is no longer a clear-cut distinction between a wave and a direct response to the forcing, nor are the waves trapped in the tropics: they give rise to global modes instead. In essence, we are looking at a meridional cross-section of the thermal tide.

In Fig. 4, we return to the baroclinic mode and the solstice, but perform a "pre-Copernican" experiment, where the frequency of the Earth's rotation and the diurnal cycle of the sun decouple. This allows us to pick $\omega = \sqrt{3}$, yielding a band of trapped waves between $-60°$ and $60°$, confirmed in the numerical results. Notice that any $\omega \geq 2$ yields global modes that extend throughout the sphere; hence no harmonic of the diurnal cycle gives rise to trapped waves. One might speculate that such higher harmonics may be components of the "teleconnections" between the tropics and the middle and high latitudes [16].
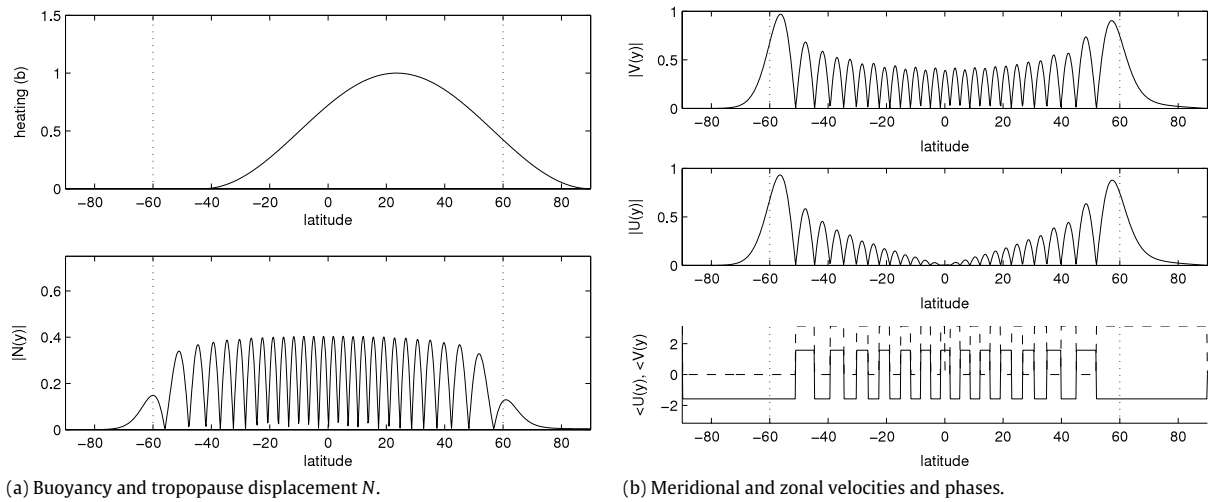
(a) Buoyancy and tropopause displacement N.

(b) Meridional and zonal velocities and phases.

Fig. 4. Linear model for non-synchronous forcing.

3.2. A nonlinear model

We return now to the nonlinear system (2)–(4), and rectify the spherical geometry, writing instead the more standard rotating shallow water equations

$$h_t + [hv]_y = 0 \tag{21}$$

$$(hv)_t + [hv^2]_y + \left[\frac{1}{2}g'h^2\right]_y + f(y)hu = 0 \tag{22}$$

$$(hu)_t + [hvu]_y - f(y)hv = 0, \tag{23}$$

or, in smooth parts of the flow,

$$h_t + vh_y + hv_y = 0 \tag{24}$$

$$v_t + vv_y + g'h_y = -f(y)u - \frac{1}{2}g'_y h \tag{25}$$

$$u_t + vu_y = f(y)v, \tag{26}$$

with

$$\frac{\mathrm{d}g'}{\mathrm{d}t} = g'_t + vg'_y = \lambda(H(y,t) - g'). \tag{27}$$

Waves in the nonlinear model will break, and thus we must impose a physically appropriate conservation law form. The nonlinear model should not really conserve volume: we expect the troposphere to adjust to violent motions by entraining and mixing stratospheric air, thus adopting its distinct, hat-shaped profile. To permit this, we replace volume by energy conservation:

$$\left[h\frac{v^2 + u^2 + g'h}{2}\right]_t + \left[v\left(h\frac{v^2 + u^2 + g'h}{2} + \frac{1}{2}g'h^2\right)\right]_y$$
$$= \frac{h^2}{2}\frac{\mathrm{d}g'}{\mathrm{d}t}. \tag{28}$$

In smooth parts of the flow, both conservation forms are equivalent. When waves break, however, we have shown in [14] that energy conservation yields volume growth, in fact maximizing entrainment among all subcritical flows that do not generate energy spontaneously at shocks. In our model, this entrainment should not be interpreted literally as the overturning of a baroclinic wave with a direct effect on the height of the troposphere, but rather as an energetically consistent approach stating that violent wave action in the troposphere eventually results in mixing and entrainment.

We solve this system numerically using a second order Godunov method [17]. Quite a few details are specific to our system, so we briefly summarize the methodology below:

- We have a vector of conserved quantities, one of the corresponding fluxes and one of the forcing terms,

$$U = \begin{pmatrix} E \\ M_v \\ M_u \end{pmatrix}, \qquad Q = \begin{pmatrix} Q_e \\ Q_v \\ Q_u \end{pmatrix} \quad \text{and} \quad F = \begin{pmatrix} F_e \\ F_v \\ F_u \end{pmatrix},$$

satisfying

$$U_t + Q_y = F.$$

Here

$$U = \begin{pmatrix} h\dfrac{v^2 + u^2 + g'h}{2} \\ hv \\ hu \end{pmatrix},$$

$$Q = \begin{pmatrix} v\left(h\dfrac{v^2 + u^2 + g'h}{2} + \dfrac{1}{2}g'h^2\right) \\ hv^2 + \dfrac{1}{2}g'h^2 \\ hvu \end{pmatrix}$$

and

$$F = \begin{pmatrix} \dfrac{h^2}{2}\dfrac{\mathrm{d}g'}{\mathrm{d}t} \\ -f(y)hu \\ f(y)hv \end{pmatrix}.$$

In order to compute the fluxes Q from the conserved quantities U, one needs to find h, which is given by the largest (i.e., positive and subcritical) solution of the cubic equation

$$E = \frac{M_v^2 + M_u^2}{2h} + g'\frac{h^2}{2}.$$

- We also have four generalized Riemann invariants: the shallow water Riemann invariants

$$R^\pm = v \pm 2\sqrt{g'h},$$

the zonal speed u, and the reduced gravity g'. In smooth parts of the flow, they satisfy the following forced characteristic equations:

$$R_t^\pm + \left(v \pm \sqrt{g'h}\right)R_y^\pm = -f\,u + \frac{1}{2}hg'_y \pm \sqrt{\frac{h}{g'}}H_g \tag{29}$$

$$u_t + v\,u_y = f\,v \tag{30}$$
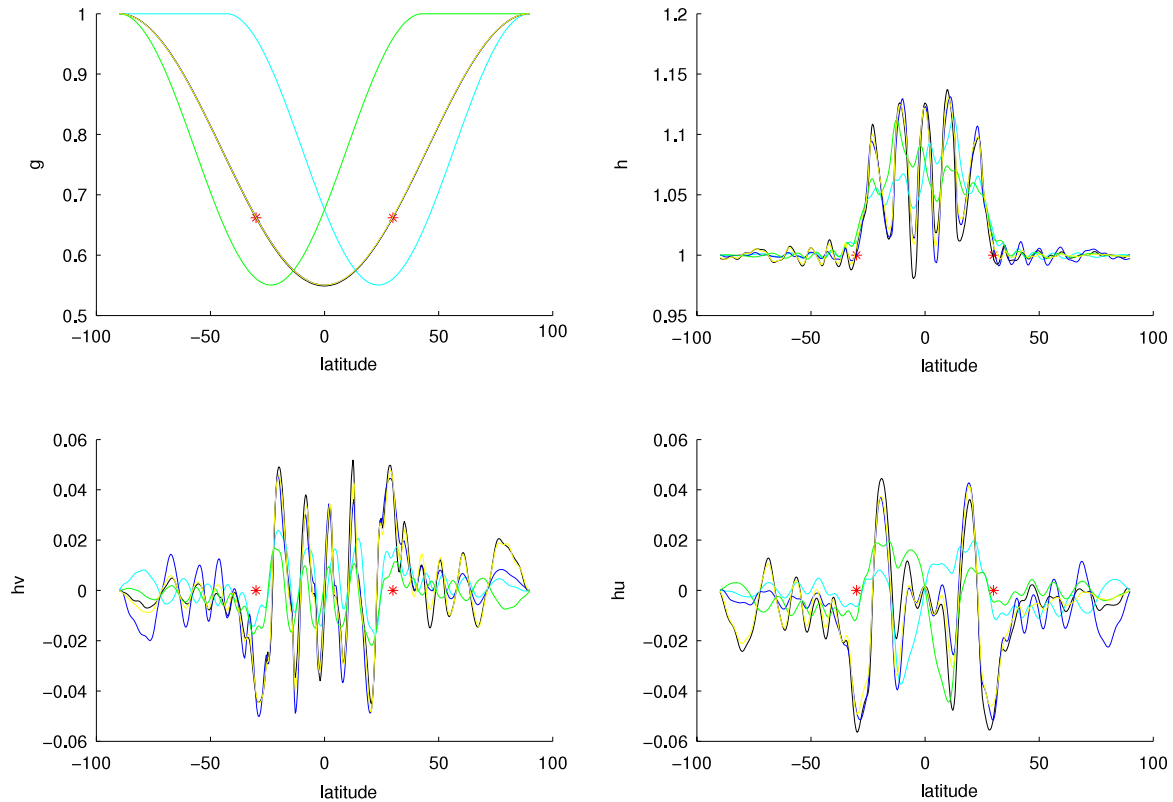
$$g'_t + v\,g'_y = H_g, \tag{31}$$

Fig. 5. Seasonal snapshots of meridional forcing of the reduced gravity field (top-left), height of the tropopause (top-right), meridional momentum (bottom-left) and zonal momentum (bottom-right). The four curves in each panel correspond to 2 solstices and 2 equinoxes of a given year.

where

$$H_g = \lambda \left(H(y, t) - g' \right)$$

is the external heating source.

- We set a regularly spaced spatial grid with cells centered at $y = y_j$ and interfaces between cells at $y = y_{j+\frac{1}{2}}$. Each time step $t = t_n$ starts with knowledge of the current mean values $(U_j^n, g_j'^n)$ of the conserved quantities U and of the reduced gravity g' over the cells, and computes these average values at time $t = t_{n+1}$. For the U's, this is done enforcing conservation and second order accuracy, in the form

$$U_j^{n+1} = U_j^n + \frac{\Delta t}{\Delta y} \left(Q_{j-\frac{1}{2}}^{n+\frac{1}{2}} - Q_{j+\frac{1}{2}}^{n+\frac{1}{2}} \right) + \frac{\Delta t}{2} \left(F_j^n + F_j^{n+1} \right), \quad (32)$$

and, for g', through

$$g_j'^{n+1} = g_j'^n + \frac{\Delta t}{2} \left(F_{g_j}^n + F_{g_j}^{n+1} \right),$$

where $F_g = H_g - v\, g_y'$.

In order to compute all the elements required for these updates, we start by computing the four Riemann invariants at the cell's centers from the conserved quantities at time t_n, and building a piecewise linear approximation to them using centered differences with van Leer slope limiters [18]. Then, tracing back the characteristics to time t_n and using the forced Eqs. (29)–(31), we solve the generalized Riemann problems (to second order in Δt), seeking the solution at each interface at $t = t_{n+\frac{1}{2}}$, halfway through the time step [19]. With these solutions, we compute the fluxes $Q_{j\pm\frac{1}{2}}^{n+\frac{1}{2}}$.

Knowing the fluxes at time $t_{n+\frac{1}{2}}$ and forces at time t_n, we can compute a first order approximation to U_j^{n+1} using (32) with both forces at time t_n (the predictor step of a *predictor–corrector*

approach). With these U's, we compute a first order approximation to the forces at time t_{n+1}, and are ready to apply formula (32) to update the U's with second order accuracy.

3.3. Nonlinear results

In the experiments below, we have adopted the thermal forcing profile (6), but with the two dominating temporal components: one daily and one steady, of comparable amplitude, as in the Fourier expansion (9). (Including the steady mode was not necessary in the linear scenario, where the various modes decouple.) It turns out, however, that the existence of free daily modes in the tropics amplifies the effect of the diurnal component enormously – in a standard resonant effect –, making by comparison the effects of the steady component almost negligible, and so effectively suppressing any significant nonlinear interaction between the two modes. (In fact, it is this resonance that explains why it is not correct to neglect the daily component of the heating. The justification typically invoked for this neglect is that the radiative relaxation time of the atmosphere is significantly longer than a day. Yet it is a well known fact that, in the presence of resonance, small forcing effects are greatly magnified.)

Since the model entrains air at breaking waves but has no detrainment mechanism, the total volume of the model troposphere increases continuously. In order to reach equilibrium balance, one could add a relaxation term that pushes the height back to its initial configuration. Such a relaxation term is added as a forcing to the energy equation (since there is no independent equation for the height) that would account for a "restratification" of the top of the troposphere. Although we have implemented this, in order not to complicate the discussion with extra forcing parameters, we report here on an experiment done without this relaxation. We simply run our model for a finite amount of time, and stop before
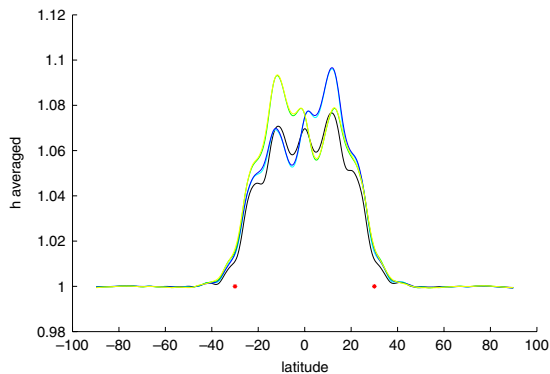
Fig. 6. Seasonal averaged tropopause height.

the tropospheric height reaches levels incompatible with the modeling assumptions.

The results of this numerical experiment are shown below. We have used the thermal forcing in (6), (7) and (10), with F limited to two frequencies: $\omega_0 = 0$, the averaged component of the forcing, and $\omega_1 = 1$, the daily component, both with amplitude $f_{0,1} = 0.3$, and a buoyancy relaxation constant $\lambda = 1$.

In Fig. 5 we see four snapshots, corresponding to the two solstices and two equinoxes of the third year of the run which started at $t = 0$ from a profile with uniform height $h = 1$ and zero velocities. Shown are the buoyancy field g' – reflecting the forcing – the height h, and the two components of the volume flow: hv and hu. Fig. 6 shows the height averaged over each of the four seasons of this third year. As in the linear case, the wave action is clearly trapped between $-30°$ and $30°$, but this wave action leads to breaking and entrainment, which in turn leads to a hat-shaped profile for h. The thermal zonal winds – the subtropical jets – prevent the tropics to spread beyond $30°$, as they would in a non-rotating planet. As in the real Earth, the location of the outer edges of the tropics, at the Horse latitudes, are season-independent.

4. Discussion

In this paper, we proposed an explanation for the meridional extent of the tropics: baroclinic diurnal waves, forced by the sun, are trapped between $-30°$ and $30°$ of latitude. On the one hand, this explains very simply why the wind field in the tropics has such marked daily signal, all but absent in most of the middle and high latitudes—when the signal is present at higher latitudes, for instance as sea-breeze in coastal areas, it is clearly as a direct local response to the forcing. In the tropics, the daily signal is global, organized in cells of diameters around 1000 km. By contrast, daily barotropic waves, responsible for the thermal tides, are not trapped: their length-scales are around 20,000 km.

We argue that this trapping of diurnal waves is also responsible for the meridional extent of the Hadley cells, whose outer edges are invariably at $\pm 30°$, the Horse latitudes, independently of the season. The reason is that wave action is responsible for much of the stirring of the tropical troposphere, not only through mixing by breaking waves, but also through the organization of the alternating areas of high and low pressure underlying large-scale convection.

To validate these ideas, we have written a simple, one-layer model of the troposphere, forced daily by the sun, which displays, at the linear level, the phenomenon of wave trapping and, nonlinearly, transforms this wave action into air entrainment, thus giving rise to a hat-shaped profile comparable to the actual tropopause. In the model, we can decouple the thermal from the mechanical day (in Venus, one is twice as long as the other)

and show how, were these to differ, the tropics would extend to latitudes other than $30°$.

In a single layer model with no return flow, there is no place for a mean meridional circulation. Thus we obtain the correct shape of the troposphere, but with no Hadley circulation underlying it. We discuss, in these last few paragraphs, what ingredients it would take to construct a simple model that could capture this circulation. Clearly, one would need at least two fluid layers: one representing the bulk of the troposphere, and the other the boundary flow. To be realistic, the boundary layer should be thinner and controlled by friction, a simple surrogate for Ekman dynamics. As in this paper, one could exclude all zonal dependence from the model (which is quite different from taking zonal means) so as to reduce its dimensionality. Lastly, an extra requirement appears necessary if one is to generate a realistic circulation: the flow should not be arrested far from its minimal energy configuration by a zonal thermal wind. For this, the model needs to include a surrogate of the baroclinic instability. It appears that the simplest model with these characteristics is that of a two-layer flow bounded above and below by rigid lids. The remaining challenge then, of course, is to develop a closure for volume exchange among the layers, possibly similar in spirit to our closure for entrainment by breaking waves.

We are currently developing one such model; we hope that, we may have it ready for Lou Howard's next birthday conference!

Acknowledgement

References

[1] I.M. Dima, J.M. Wallace, On the seasonality of the Hadley cells, J. Atmospheric Sci. 60 (2003) 1522–1527.

[2] I.M. Held, A.Y. Hou, Nonlinear axially symmetric circulations in a nearly inviscid atmosphere, J. Atmospheric Sci. 37 (1980) 515–533.

[3] I.M. Held, The general circulation of the atmosphere, Notes of the WHOI GFD Summer School, 2000.

[4] Y. Hu, Q. Fu, Observed poleward expansion of the Hadley circulation since 1979, Atmos. Chem. Phys. 7 (2007) 5229–5236.

[5] J. Lu, G.A. Vecchi, T. Reichler, Expansion of the Hadley cell under global warming, Geophys. Res. Lett. 34 (2007).

[6] D.J. Seidel, W.J. Randel, Recent widening of the tropical belt: evidence from tropopause observations, J. Geophys. Res. 112 (2007).

[7] D.J. Seidel, Q. Fu, W.J. Randel, T.J. Reichler, Widening of the tropical belt in a changing climate, Nat. Geosci. 1 (2008) 21–24.

[8] S.S. Chen, A. House Jr., Diurnal variation and life-cycle of deep convective systems over the tropical Pacific warm pool, Q. J. R. Meteorol. Soc. 123 (1997) 357–388.

[9] K. Imaoka, R.W. Spencer, Diurnal variation of precipitation over the tropical oceans observed by TRMM/TMI combined with SSM/I, Amer. Meteor. Soc. 13 (2000) 4149–4158.

[10] M. Wheeler, G.N. Kiladis, Convectively coupled equatorial waves: analysis of clouds and temperature in the wavenumber frequency domain, J. Atmospheric Sci. 56 (1999) 374–399.

[11] D.M.W. Frierson, J. Lu, G. Chen, Width of the Hadley cell in simple and comprehensive general circulation models, Geophys. Res. Lett. 34 (2007).

[12] T. Schneider, The general circulation of the atmosphere, Annu. Rev. Earth Planet. Sci. 34 (2006) 655–688.

[13] G.K. Vallis, Atmospheric and Oceanic Fluid Dynamics, Cambridge University Press, 2006.

[14] T. Jacobson, P.A. Milewski, E.G. Tabak, Mixing closures for conservation laws in stratified flows, Stud. Appl. Math. (2007).

[15] O. Buhler, Equatorward propagation of inertia-gravity waves due to steady and intermittent wave sources, J. Atmospheric Sci. 60 (2003) 1410–1419.

[16] A.M. Grimm, P.L. Silva Dias, Analysis of tropical-extratropical interactions with influence functions of a barotropic model, J. Atmospheric Sci. 52 (1995) 3538–3555.

[17] S.K. Godunov, A difference scheme for numerical solution of discontinuous solution of hydrodynamic equations, Mat. Sb. 47 (1959) 271–306. (Translated US Joint Publ. Res. Service, JPRS 7226, 1969).

[18] B. van Leer, Towards the ultimate conservative difference scheme, V. A second order sequel to Godunov's method, J. Comput. Phys. 32 (1979) 101–136.

[19] E.G. Tabak, A second order Godunov method on arbitrary grids, J. Comput. Phys. 124 (1996) 383–395.